J Mater Sci (2007) 42:3223–3229
DOI 10.1007/s10853-006-0238-x

Mechanical properties for bulk metallic glass with crystallites precipitation and second ductile phase addition

Ke-Qiang Qiu · D. Z. Hao · Y. L. Ren · H. Zhang

Received: 3 April 2005 / Accepted: 14 April 2006 / Published online: 15 January 2007

Abstract Monolithic phase bulk metallic glasses (BMGs) produced by a copper mold casting method and BMG composites containing in-situ brittle crystallites and out-situ tungsten fiber produced by a water quenching method were obtained. Mechanical properties including cyclic deformation and fracture toughness were investigated. Under symmetrically cyclic stress control, the life of tungsten fiber reinforced amorphous alloy is much longer than that of the monolithic amorphous alloy. The composite containing tungsten fibers that retard the crack propagation exhibits cyclic softening while the partially crystallized amorphous alloy exhibits stable cycling. The regions of crack initiation, stable propagation and final fracture were observed on the fracture surface. Crystalline brittle phases do not retard the crack propagation but become sites of crack initiation. Tungsten fiber reinforced BMG has the largest fracture toughness while BMG with quenched-in crystallites the smallest. Tungsten fibers stabilize crack growth in the matrix and extend the strain to failure of the composite, while brittle crystallites speed up the crack propagation even though they act as obstacles when shear bands reach them in some cases.

K.-Q. Qiu (✉) · Y. L. Ren
School of Materials Science and Engineering, Shenyang University of Technology, Shenyang 110023, China
e-mail: kqqiu@yahoo.com.cn

D. Z. Hao
Liaoning Institute of Technology, Jinzhou 121001, China

H. Zhang
Shenyang National Laboratory for Materials Science, Institute of Metal Research, Chinese Academy of Sciences, Shenyang 110016, China

Introduction

In the decades that have passed since the synthesis of the first metallic glass Au–Si by Duwez in 1960 [1], a great number of metallic glasses have been developed. Until the late 1980s, however, metallic glasses have been produced only as thin ribbon samples of a few tens micrometer thickness by melt spinning; only for some Pt and Pd alloys a relatively large size of bulk form could be produced [2–7]. Such a small size of the materials has limited their application for practical purposes. It has also limited the scientific researches on their mechanical properties. It is known that monolithic metallic glasses deform plastically by localized slips at room temperature, and the final strain is determined by the numbers of shear bands activated during deformation. Although the local plastic strain in one shear band is quite large, only a few shear bands are active before failure, which leads to catastrophic failure under unconstrained conditions without much macroscopic plasticity [8–12]. As a result, monolithic metallic glasses exhibit only a limited plastic flow under compressive or tensile loading [13–15]. The lack of ductility results in a rather limited fracture toughness [16–18], which is a critical parameter for structural materials, has limited the application of bulk metallic glasses (BMGs) as engineering materials. To improve the ductility or toughness is, to some extent, to initiate and propagate the shear bands, or to create multiple shear band formation.

A monolithic metallic glass is a disordered structure in nature. But second crystalline phases imbedded in the amorphous matrix are often detected when fabricating a metallic glass due to its low glass forming ability or crystalline inclusions. A lot of effort was

paid to the reduction of such crystalline phases due to their brittleness. We have not observed the second ductile crystalline phase effect until Leng [19] deformed the laminated composite under tensile loading, He found that a high density of multiple shear bands were formed and overall plastic tensile strain of the order of 10% could be achieved. This shows the possibility of creating multiple shear bands under loading by ''trapping'' shear band propagation between the ductile metal layers. Now many investigations [20–23] on the effect of second phases imbedded in the amorphous matrix were made in order to use BMGs as structural engineering materials. The second crystalline phases now are often introduced into the amorphous matrix to modify BMGs' microstructure. For μm scale crystallites, the two kinds of phases, i.e., ductile and brittle, are often related. The crystalline phases existed in amorphous matrix, caused by a insufficient cooling when solidifying or/and crystalline inclusions presented in the melt before casting, are usually intermetallics which are often brittle except for the special design microstructure such as a dendrtic α-Ti-type phase embedded in a BMG matrix [23, 24]. Another route to control shear band propagation is to prepare a BMG matrix composite with micrometer-sized second phase addition (particles or fibers) as a kind of reinforcement [20–22]. If a second crystalline phase is introduced into glass formation melt, the possibility of crystallization of some intermetallics increases. It is necessary to compare the mechanical properties for both cases. In this paper, we will review our recent results on mechanical properties for BMGs and BMGs with second crystalline phases in their matrix.

Experimental

The $Zr_{41.25}Ti_{13.75}Ni_{10}Cu_{12.5}Be_{22.5}$ alloy developed by Peker and Johnson [25] was used due to its high glass forming ability. The master alloys were prepared by arc melting of pure Zr, Ti, Ni, Cu and Be elements in an argon atmosphere. Two methods of sample preparation were used. One was mold casting by which master alloy was remelted in a quartz tube and injected into copper mold cavities of 4×6 mm^2 and 15×5 mm^2 in cross section with 70 mm in length. Tungsten fiber (250 μm in diameter) reinforced BMG composites as well as BMG with quenched-in crystallites using the same sizes as those prepared by copper mold casting were obtained by melt infiltration casting and water quenching methods which are described in the literature [26]. The volume fraction (V_f) of quenched-in crystallites was 3% as determined by image analysis, while the V_f for the tungsten fiber in the BMG matrix was about 10% for the samples prepared by water quenching methods. Fatigue samples were cut from the ingots using an electro-discharge machine. They were sanded and then electrolytically polished in a solution of 10% perchloric acid/90% acetic acid at room temperature. Cyclic fatigue tests were performed in a computer controlled MTS 810 series servo-hydraulic test system. The dumbbell shaped plate samples were prepared with a 10 mm gauge length. The cross section was 3×3 mm^2. In the fatigue test, a sinusoidal waveform with zero mean force [$R = -1$] was adopted at a frequency of 1 Hz. The tensile and compressive peak strains were continuously recorded for every cycle throughout the testing by an extensometer with 8 mm gauge length, clamped to the specimen. All the samples finally failed under cyclic deformation.

The experiments of fracture toughness were performed using a Shimadzu 500N servo-hydraulic test machine under displacement control with a displacement rate of 0.25 mm/s. The specimens used for fracture toughness experiments are 3-point bending samples with $4W$ gauge length, and a single edge notched with a radius and a length of 0.08 mm and $0.3W$, respectively, where W is the width of specimens. Fracture toughness calculation can be found in the standard of ASTM E-399-90.

For each experiment, at least three specimens were tested. The fracture surfaces of tested specimens were investigated using an Oxford scanning electron microscope operating at 20 kV. Secondary electron imaging was exclusively used in the present study.

Results and discussions

Microstructure of prepared specimens

Figure 1 shows the microstructure of as-cast specimens. The sample produced by copper mold casting exhibits a structureless microstructure (Fig. 1a). While some crystallites are generally precipitated for those with and without tungsten reinforced samples produced by the water quenching method as shown in Fig. 1(b) and (c). Two kinds of crystallites can be seen: one is needle-like characteristic of Be-rich Laves phase with the hcp ''$MgZn_2$–type'' structure which corresponds to previous analysis [27] and the other is dotted shape crystallites with

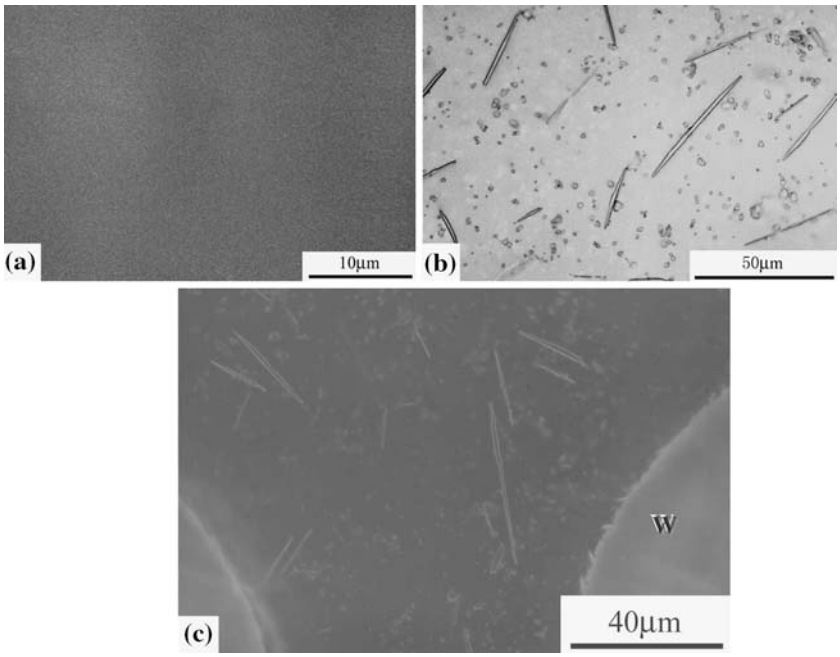

Fig. 1 Microstructures of as-cast $Zr_{41.25}Ti_{13.75}Ni_{10}Cu_{12.5}Be_{22.5}$ alloy obtained by (**a**) copper mould casting, (**b**) water quenching and (**c**) melt infiltration casting methods, respectively

"Al_2Cu-type" structure as well as an unidentified phase [28, 29].

Cyclic deformation behaviors

Figure 2 shows strain responses of single phase BMG, BMG with quenched-in crystallites and tungsten reinforced BMG matrix composite under symmetrically cyclic stress. The stress amplitude of 550 MPa for tungsten fiber reinforced composite is much lower than the yield stress of single phase BMG and BMG with quenched-in crystallites. It is well known that the strain value has a reciprocal relationship with the elastic modulus of a sample, the higher the modulus, the smaller the strain. Tungsten fiber reinforced BMG has the largest elastic modulus, therefore it has the lowest strain amplitude. The fatigue life of the monolithic BMG was longer than that of the BMG with quenched-in crystallites. Neither hardening nor softening was observed during cyclic loading. Such a stable strain response to load is due to the lack of work hardening in the structure such as the propagation of dislocation in the crystalline metal. Tungsten fiber reinforced BMG matrix composite shows more than double the fatigue life under the same conditions, and exhibits a stable fatigue softening which implies that a long crack may stably propagate which results in the increase of flexibility of the fatigue sample.

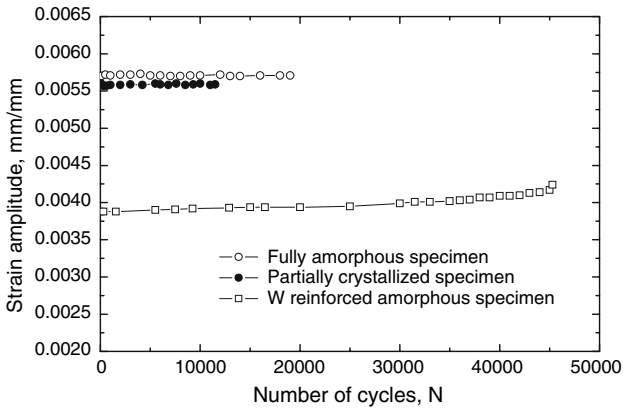

Fig. 2 Strain response in bulk metallic glass under symmetrically cyclic stress

The morphologies of fatigue fracture surfaces were examined to reveal the relationship between the fatigue-crack initiation, growth and the strip marks or striations. Figure 3 shows the macro-fracture surfaces of the three materials. The fracture planes for each specimen are perpendicular to their applied load. The fracture surface from the specimen with quenched-in crystallites shows flattened morphology. The other two show a fluctuant surface, which needs more energy to cause a fracture. Each fracture surface is classified into three stages. In the first stage, the initiation of cracks occurred at the surface with a tiny pore caused by the solidification process (for single phase BMG) or the quenched-in crystalline particle (for the BMG with quenched-in crystallites and tungsten fibers). Figure 4 shows the fatigue-crack initiation areas. A tiny pore and a quenched-in crystallite are the sources for the fatigue cracking for single phase BMG as well as for

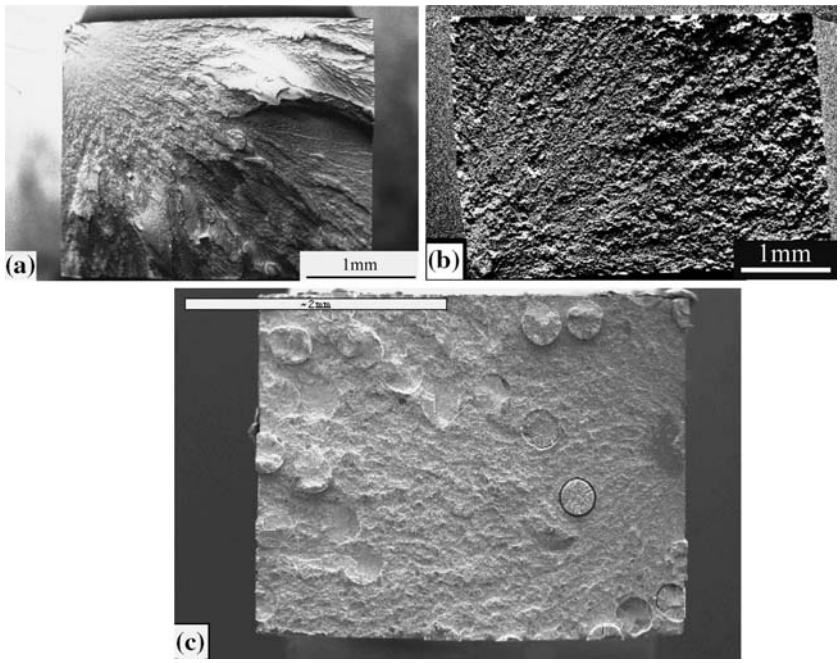

Fig. 3 Macro-fracture surface for (**a**) monolithic BMG, (**b**) BMG with quenching-in crystallites and (**c**) tungsten reinforced BMG under symmetrically cyclic stress

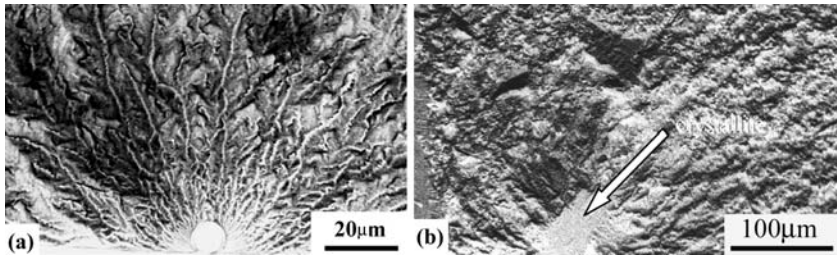

Fig. 4 Fatigue-crack initiation areas for (**a**) single phase BMG as well as (**b**) BMG with quenched-in crystallites

the composites. In the second stage, fatigue cracks propagated stably with the formation of some plateaus, the quite large propagation area and the face to face slip for tungsten reinforced BMG are also the reason why it has the longest fatigue lifetime. In the third stage, the cracks propagated unstably through the sample abruptly. Figure 5a shows the three fatigue-fractured stages for single phase BMG marked by

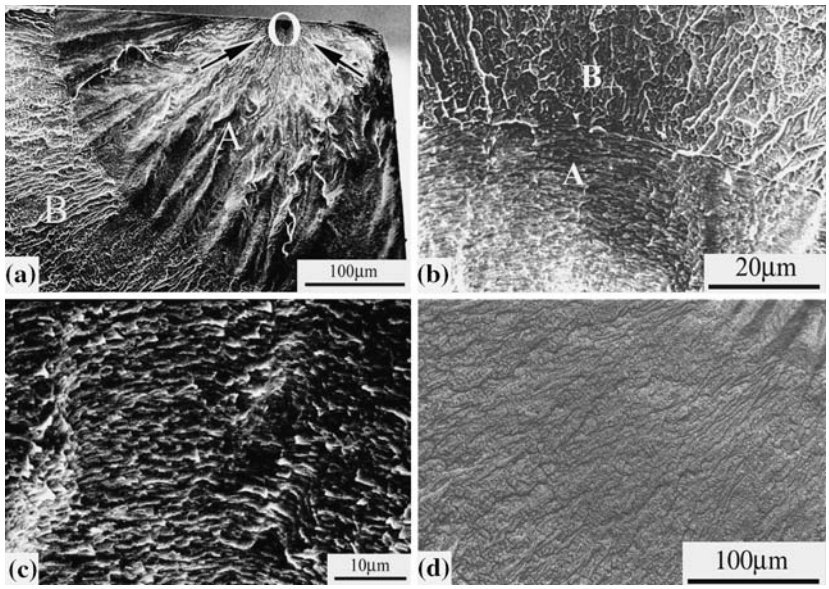

Fig. 5 The overall fatigue fracture surface for monolithic phase BMG (**a**), the marked line between stable crack propagation area (marked with A) and unstable crack propagation area (marked with B) (**b**), ordered stripe marked with concentric circles, the spacing between the stripe is about 0.3–0.4 μm (**c**), unstable fatigue crack propagation region (**d**)

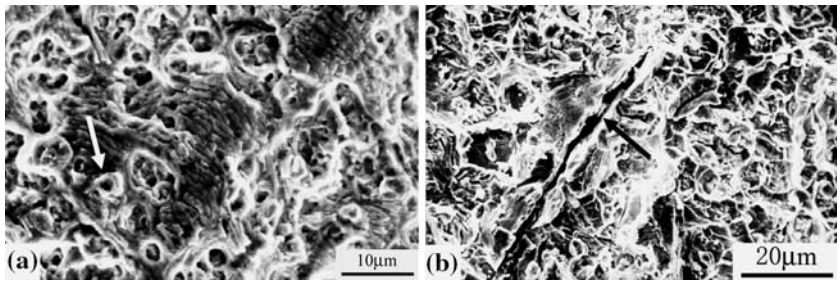

Fig. 6 Fatigue fracture surface for BMG with quenched-in crystallites with (**a**) cyclic striations and (**b**) a needle-like crystallite on the fracture surface

arrows (or letter O), **A** and **B,** respectively. Around the tiny pore there exists a mirror zone (not shown) which was also observed in the fatigue initiation area of $Zr_{55}Al_{10}Ni_5Cu_{30}$ BMG [30]. This was caused by cyclic rubbing of cracking surfaces. The image shown in Fig. 5b indicates the distinct difference of morphologies between the second (**A**) and third (**B**) stages. The **A** is believed to be a stable fatigue crack growth area forming ordered stripes marked by concentric circles which are similar to that observed in ductile crystalline metals. The spacing between the stripes is about 0.3–0.4 μm (Fig. 5c). The area **B** is an unstable fatigue crack propagation region that runs quickly through the cross-section of the sample; the morphology of this area shows a venous pattern typical of swift movement of the fracture surface of BMG during shear flowing (Fig. 5d). In the sample with quenched-in crystallites, the distinction between the stable fatigue crack propagation area and the transient fracture area is not as obvious as the case in the monolithic BMG, as is shown in Fig. 6. The quenched-in crystallites were clearly seen on the fracture surface as indicated by arrows. Though the cyclic striation can be observed in the stable fatigue fracture propagation area (Fig. 6a), the propagation direction is blurry. This may be caused by the connection of the initial cracks of the quenched-in crystallites through propagation before the host crack arrives under loading. Most of the fatigue-fracture area belongs to the transient fracture area. Therefore, the sample exhibits a short fatigue lifetime. The particles, especially needle-like crystallites indicated by an arrow in Fig. 6b act as a crack in the matrix. They allow the propagation of the fatigue cracks to quickly pass without retarding effect due to the brittle nature of those intermetallics. Their lifespan is thus reduced.

Although the uneven distribution of tungsten fibers in the amorphous matrix (shown in Fig. 3c) a long fatigue lifetime was obtained in such composite. Cracks initiated from some weak sites and then began to propagate forwards forming a stable propagation area. Fatigue striations on the enlarged image shown in Fig. 7a are similar to that of BMG with quenched-in crystallites. Figure 7b shows a typical area around tungsten fibers on the fatigue fracture surface. A few of tungsten fibers were debonded from the matrix due to action between crack tips and the tungsten fibers during cyclic loading. This debonding process, which occurred in the stable propagation cracking area, would blunt the cracking tips and increase the flexibility of the sample. Therefore, a relatively large stable propagation area was obtained compared with those of the other two materials. The unstable or transient fatigue area is similar to that of the specimen with quenched-in crystallites.

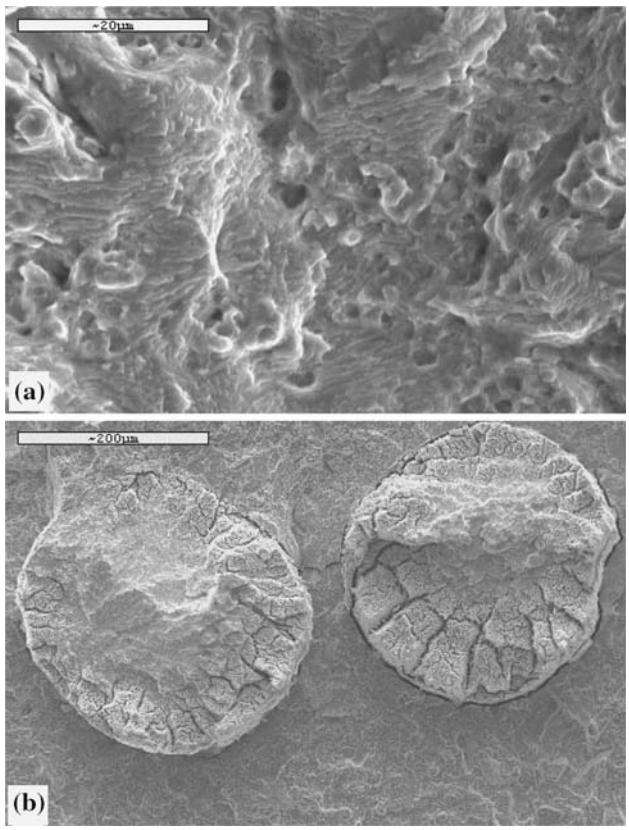

Fig. 7 Fracture surface for tungsten fiber reinforced BMG with (**a**) stable propagation area and (**b**) the fibers in the matrix after cyclic loading

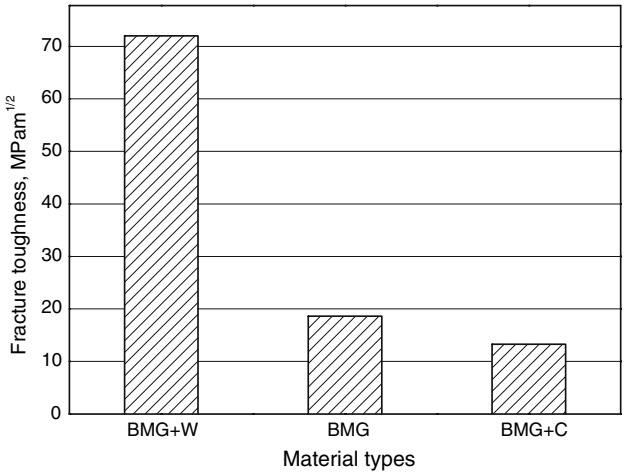

Fig. 8 Fracture toughness for BMG, BMG containing quenched-in crystallites (BMG+C) and BMG reinforced by tungsten fibers (BMG+W), respectively

Fracture toughness

The values of fracture toughness are shown in Fig. 8 where it is clearly seen that the tungsten fiber reinforced BMG has relatively the largest fracture toughness, while the BMG with quenched-in crystallites the smallest. Figure 9 shows the crack propagation path for the two composites. The fracture propagation path for monolithic BMG is similar with that of BMG with quenched-in crystallites. All the values obtained by 3-point bending are lower than that observed by Flores [31] who used single edge notched fracture sample loaded in tension in her experiments, in which fracture toughness in excess of 130 MPa$\sqrt{m}$ were found. These high values were believed to be associated with significant crack tip plastic deformation and blunting. Localized shear bands and branched cracks form an energy dissipation damage zone at the crack tip. We have not observed such a distributed damage zone in both the monolithic BMG and BMG with quenched-in crystallites due to the different experimental method. However, a similar phenomenon, i.e., branching and blunting, was observed in the tungsten fiber reinforced sample (Fig. 9b). The blunting by the tungsten was due to its plastic deformation and branching with further cyclic loading dissipating the energy of the damage zone. Therefore, it is not difficult to understand why tungsten fiber reinforced BMG has the highest values of fracture toughness.

The above experiments have shown that reinforcing BMG with tungsten fiber can improve the mechanical properties of the material regarding fatigue and 3-point bending, whereas the brittle crystallites in the amorphous matrix caused by insufficient cooling or low glass forming ability of melt are often unexpected due to making those properties deteriorated. Our previous experiments have also shown that reinforcing BMG with tungsten fibers can improve plastic deformation in tension and compression [32] and increase the energy of Charpy impact [33] by restricting shear bands propagation, promoting the generation of multiple shear bands, increasing additional fracture surfaces and bridging effect between the reinforcement and matrix. In cyclic loading and three-point bending experiments, the plastic deformation of tungsten fiber increases the flexibility of the samples in face to face slipping and long crack propagation by dissipating the energy of crack-tips in the damage zone and by increasing the stable propagation area. Therefore, reinforcing BMG with ductile crystallites can be regarded as an important way to improve the mechanical properties of BMGs.

Conclusion

Three kinds of BMG related materials, i.e., a monolithic phase BMG, BMG with quenched-in crystallites and ductile tungsten fibers were fabricated. Mechanical properties, including cyclic deformation and fracture toughness were investigated. Under symmetrically cyclic stress control, the life of tungsten fiber reinforced amorphous alloy was much longer than that of the monolithic amorphous alloy. Tungsten fiber could retard crack propagation. The composite containing tungsten fibers exhibited cyclic softening while the partially crystallized amorphous alloy exhibited stable

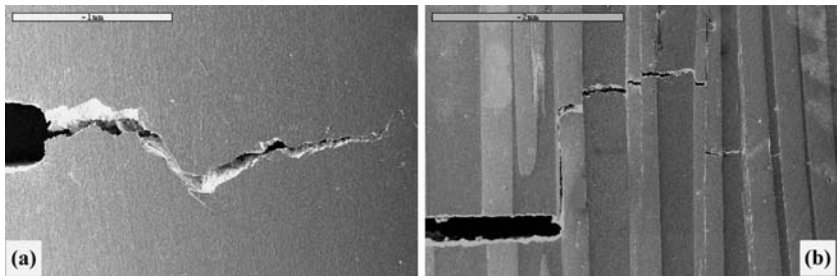

Fig. 9 Crack propagation for BMG (**a**) and BMG reinforced by tungsten fiber (**b**) under three-point bending test

cycling. The region of crack initiation, stable propagation and final fracture can be observed on the fracture surface. Crystalline brittle phases could not retard the crack propagation but became sites of crack initiation. The tungsten fiber reinforced amorphous composites possess the highest fracture toughness which originates from its blunting and branching in the damage zone.

References

1. Klement W, Willens RH, Duwez P (1960) Nature 187:869
2. Chen HS, Turnbull D (1969) Acta Metall 17:1021
3. Steinberg J, Lord AE, Lacy LL, Johnson J (1981) Appl Phys Lett 38:135
4. Lee MC, Kendall JM, Johnson WL (1982) Appl Phys Lett 40:382
5. Drehman AJ, Greer AL, Turnbull D (1982) Appl Phys Lett 41:16
6. Kui HW, Greer AL, Turnbull D (1984) Appl Phys Lett 45:615
7. Inoue A, Ekimoto T, Masumoto T (1988) Int J Rapid Solidifact 3:237
8. Bruck HA, Christman T, Posakis AJ, Johnson WL (1994) Scripta Metall Mater 30:429
9. Bruck HA, Rosakis AJ, Johnson WL (1996) J Mater Res 11:503
10. Alpas AT, Embury JD (1988) Scripta Metall Mater 22:256
11. Hufnagel TC, El-Deiry P, Vince RP (2000) Scripta Mater 43:1071
12. Pampillo CA (1975) J Mater Sci 10:1194
13. Leonhard A, Xing LQ, Heimaier M, Gebert A, Eckert J, Schultz L (1998) Nanostruct Mater 10:805
14. Fan C, Li C, Inoue A, Haas V (2000) Phys Rev B 61:3761
15. Bertrand C, Xing LQ, Dallas JP, Cornet M (1998) Mater Sci Eng A 241:216
16. Gilbert CJ, Ritchie RO, Johnson WL (1997) Appl Phys Lett 71:476
17. Conner RD, Rosakis AJ, Johnson WL, Owen DM (1997) Scripta Metall Mater 37:1373
18. Lowhaphandu P, Lewandoski JJ (1998) Scripta Metall Mater 38:1811
19. Leng Y, Courtney TH (1991) J Mater Sci 26:588
20. Choi-Yim H, Johnson WL (1997) Appl Phys Lett 71:3808
21. Conner RD, Dandliker RB, Johnson WL (1998) Acta Mater 46:6089
22. Choi-Yim H, Busch R, Köster U, Johnson WL (1999) Acta Mater 41:2455
23. Eckert J, Kühn U, Mattern N, He G, Gebert A (2002) Intermetallics 10:1183
24. Kühn U, Eckert J, Mattern N, Schultz L (2002) Appl Phys Lett 80:2478
25. Peker A, Johnson WL (1993) Appl Phys Lett 63:2342
26. Qiu KQ (2002) PhD Dissertation, Institute of Metal Research, Chinese Academy of Sciences
27. Schneider SP, Thiyagarajan P, Johnson WJ (1996) Appl Phys Lett 68:493
28. Busch R, Schneider SP, Peter A, Johnson WJ (1995) Appl Phys Lett 67:1544
29. Fecht HJ (1997) Phil Mag B 76:495
30. Yokoyama Y, Fukaura K, Sunada H (2000) Mater Trans JIM 40:675
31. Flores KM, Dauskardt RH (1999) Scripta Metall Mater 41:937
32. Qiu KQ, Wang AM, Zhang HF, Ding BZ, Hu ZQ (2002) Intermetallics 10:1283
33. Qiu KQ, Wu XF, Wang AM, Zhang HF, Ding BZ, Hu ZQ (2003) Metall MaterTrans A 34A:1147